J|A|C|S ARTICLES

Published on Web 10/25/2010

Phthalocyanine−Pyrene Conjugates: A Powerful Approach toward Carbon Nanotube Solar Cells

Juergen Bartelmess,[†] Beatriz Ballesteros,[‡] Gema de la Torre,[‡] Daniel Kiessling,[†] Stephane Campidelli,[#,||] Maurizio Prato,*[,#] Tomás Torres,*[,‡,§] and Dirk M. Guldi*[,†]

Department of Chemistry and Pharmacy and Interdisciplinary Center for Molecular Materials, Friedrich-Alexander-University Erlangen-Nuremberg, 91058 Erlangen, Germany, Departamento de Química Orgánica, Universidad Autónoma de Madrid, Cantoblanco, 28049 Madrid, Spain, Center of Excellence for Nanostructured Materials and INSTM, Unit of Trieste, Dipartimento di Scienze Farmaceutiche, University of Trieste, Piazzale Europa 1, 34127 Trieste, Italy, and IMDEA Nanociencia, Facultad de Ciencias, Cantoblanco, 28049 Madrid, Spain

Received August 9, 2010; E-mail: tomas.torres@uam.es; dirk.guldi@chemie.uni-erlangen.de

Abstract: In the present work, a new family of pyrene (Py)-substituted phthalocyanines (Pcs), i.e., ZnPc-Py and H_2Pc-Py, were designed, synthesized, and probed in light of their spectroscopic properties as well as their interactions with single-wall carbon nanotubes (SWNTs). The pyrene units provide the means for non-covalent functionalization of SWNTs via $\pi-\pi$ interactions. Such a versatile approach ensures that the electronic properties of SWNTs are not impacted by the chemical modification of the carbon skeleton. The characterization of ZnPc-Py/SWNT and H_2Pc-Py/SWNT has been performed in suspension and in thin films by means of different spectroscopic and photoelectrochemical techniques. Transient absorption experiments reveal photoinduced electron transfer between the photoactive components. ZnPc-Py/SWNT and H_2Pc-Py/SWNT have been integrated into photoactive electrodes, revealing stable and reproducible photocurrents with monochromatic internal photoconversion efficiency values for H_2Pc-Py/SWNT as large as 15 and 23% without and with an applied bias of +0.1 V.

Introduction

Organic photovoltaics has emerged as a major topic in contemporary research.[1] Importantly, the basic *modus operandi* for most approaches toward organic photovoltaics is taken from natural photosynthesis, that is, electron donor−acceptor interactions. To this end, the radical ion pair states, which are generated upon photoexcitation followed by charge separation, are utilized to inject charge carriers (i.e., electrons and holes) into electrodes (i.e., anodes and cathodes) that lead eventually to the production of electric currents. The realization of organic photovoltaics is based on, for example, the use of semiconducting polymers including poly(*p*-phenylenevinylene) and polythiophene.[2] Owing to the outstanding electron acceptor features of C_{60} and its derivatives, strategies have been developed to blend them into polymer matrices in a bulk heterojunction configuration to enhance the overall photoactive performance.[3] Dyes such as phthalocyanines (Pcs) and porphyrins have been studied as light-harvesting units, especially in organic planar heterojunction solar cells[4] and for the sensitization of mesoscopic semiconductors.[5]

With regard to novel electron donor−acceptor conjugates/hybrids, emphasis is placed on carbon nanotubes, in general, and single-wall carbon nanotubes (SWNTs), in particular. Carbon-based nanomaterials are currently under active investigation for producing innovative materials, composites, and electronic devices of greatly reduced size.[6] In particular, SWNTs are one-dimensional nanowires that readily accept charges, which can then be transported along their tubular axis. The electrical conductivity, morphology, and good chemical stability of SWNTs are promising features that stimulate their integration into electronic devices.[7] To date, SWNTs have been shown to act as electron acceptors when adequately interfaced with excited-state electron donors.[8] Interfacing SWNTs with electron

[†] Friedrich-Alexander-University Erlangen-Nuremberg.
[‡] Universidad Autónoma de Madrid.
[#] University of Trieste.
[§] IMDEA Nanociencia.
[||] Present address: Laboratoire d'Electronique Moléculaire, CEA Saclay.

(1) Special issue on "Artificial Photosynthesis and Solar Fuels". *Acc. Chem. Res.* **2009**, *42*, 1859−2029.
(2) (a) Cheng, Y.-J.; Yang, S.-H.; Hsu, C.-S. *Chem. Rev.* **2009**, *109*, 5868. (b) Chen, J.; Cao, Y. *Acc. Chem. Res.* **2009**, *42*, 1709.
(3) Dennler, G.; Scharber, M. C.; Brabec, C. J. *Adv. Mater.* **2009**, *21*, 1323, and references cited therein.
(4) Bottari, G.; de la Torre, G.; Guldi, D. M.; Torres, T. *Chem. Rev.* **2010**, DOI: 10.1021/cr900254z and references cited therein.
(5) (a) Reddy, Y.; Giribabu, L.; Lyness, C.; Snaith, H.; Vijaykumar, C.; Chandrasekharam, M.; Lakshmikantam, M. J.; Yum, H.; Kalyanasundaram, K.; Grätzel, M.; Nazeeruddin, M. K. *Angew. Chem., Int. Ed.* **2007**, *46*, 373. (b) Cid, J.-J.; Yum, J.-H.; Jang, S.-R.; Nazeeruddin, M. K.; Martínez-Ferrero, E.; Palomares, E.; Ko, J.; Grätzel, M.; Torres, T. *Angew. Chem., Int. Ed.* **2007**, *46*, 8358. (c) Imahori, H.; Umeyama, T.; Ito, S. *Acc. Chem. Res.* **2009**, *42*, 1809. (d) Mori, S.; Nagata, M.; Nakahata, Y.; Yasuta, K.; Goto, R.; Kimura, M.; Taya, M. *J. Am. Chem. Soc.* **2010**, *132*, 4054. (e) Martínez-Díaz, M. V.; Torres, T. In *Handbook of Porphyrin Science*; Kadish, K. M., Smith, K. M., Guilard, R., Eds.; Academic Press: San Diego, 2010; Vol. 10, pp 45−141.
(6) (a) Baughman, R. H.; Zakhidov, A. A.; de Heer, W. A. *Science* **2002**, *297*, 787. (b) Thostenson, E. T.; Ren, Z.; Chou, T.-W. *Compos. Sci. Technol.* **2001**, *61*, 1899. (c) Ajayan, P. M.; Schadler, L. S.; Giannaris, C.; Rubio, A. *Adv. Mater.* **2000**, *12*, 750.
(7) (a) Ago, H.; Petritsch, K.; Shaffer, M. S. P.; Windle, A. H.; Friend, R. H. *Adv. Mater.* **1999**, *11*, 1281. (b) Tans, S. J.; Verschueren, A. R. M.; Dekker, C. *Nature* **1998**, *393*, 49.

 10.1021/ja107131r

Scheme 1. Synthesis of H_2Pc-Py and ZnPc-Py

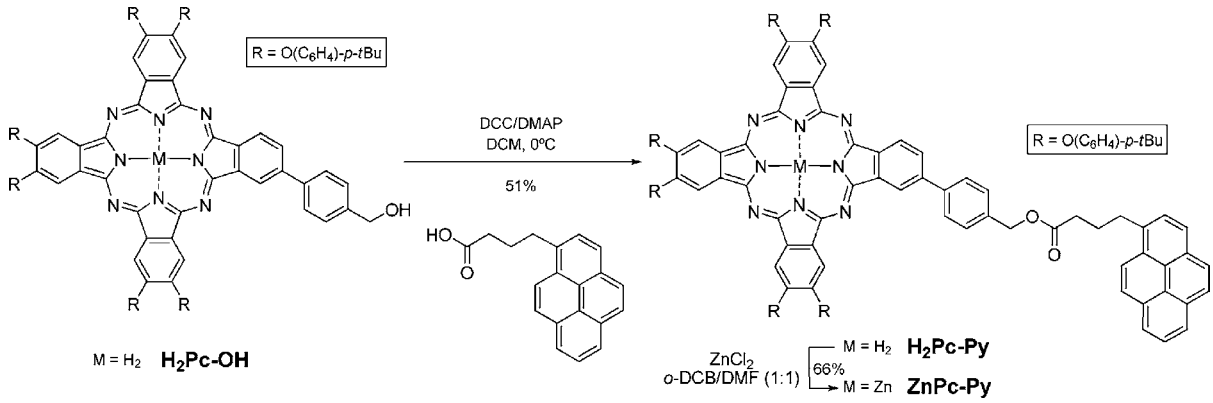

donors requires electronic communication between the different constituents via functionalization. The functionalization of SWNTs is achieved by either covalent or non-covalent chemistry. Covalent functionalization generally includes the oxidation of SWNTs to remove their caps and to create defect sites (i.e., COOH groups) at their ends as well as sidewalls. Defect sites are useful to add functional entities in subsequent steps via the formation of covalent bonds with electron donors.[9] Ultrasonic treatment can likewise induce SWNT oxidation.[10] All of these processes have in common that the rather harsh conditions cause defects on the carbon backbone of SWNTs.[11] Undeniably, such treatments influence the electronic properties of SWNTs due to partial saturation/destruction of the extended π-system. In the context of non-covalent functionalization, interactions between aromatic groups and sidewalls of SWNT are promoted by means of hydrophobic, π-stacking, or even van der Waals interactions.[8b,12] The major advantage of the non-covalent functionalization is the fact that the carbon backbone is not damaged and the properties of SWNTs are largely preserved. Leading examples include the immobilization of pyrene,[13] anthracene,[14] and porphyrins.[15]

In this study, we pursue the non-covalent immobilization of phthalocyanines as excited electron donors onto SWNTs. Phthalocyanines show excellent light-harvesting properties in the visible and NIR region of the solar spectrum as well as high photostability and unique physical properties.[16] Electron donor−acceptor interactions with phthalocyanines have been studied in many forms: phthalocyanine/porphyrin conjugates,[17] phthalocyanine/fullerene conjugates and hybrids,[4,18] as well as phthalocyanine oligomers.[19] Covalently linked Pc-SWNT ensembles have also been described.[20] The general concept of non-covalent functionalization was recently extended to probe the interactions between phthalocyanine-based poly(phenylene vinylene) oligomers and SWNTs.[21] In stark contrast to any of the aforementioned examples, we took advantage of the well-known features of pyrene and pyrene derivatives to adhere to SWNTs[13] and used them as anchor groups to immobilize metal-free (H_2Pc) as well as zinc phthalocyanines (ZnPc) onto the surface of SWNTs. The resulting electron donor−acceptor hybrids form stable suspensions in organic solvents that render them particularly useful for the production of prototype solar cells containing SWNT buckypaper—a matrix film of individual and thin bundles of SWNTs.[20f]

Synthesis

Scheme 1 summarizes the synthesis of metal-free phthalocyanine-pyrene (H_2Pc-Py) and zinc phthalocyanine-pyrene (ZnPc-Py) derivatives. Starting from the metal-free, unsymmetrically substituted Pc bearing a hydroxymethyl moiety (i.e., H_2Pc-OH),[22] an esterification reaction was carried out with 1-pyrenebutyric acid in the presence of dicyclohexylcarbodiimide (DCC) and *N*,*N*-dimethylaminopyridine (DMAP) as condensation agents. The resulting H_2Pc-Py is also the precursor of the metalated ZnPc-Py derivative, which was prepared by treatment of the metal-free conjugate with

(8) (a) Dyke, C. A.; Tour, J. M. *J. Phys. Chem. A* **2004**, *51*, 11151. (b) Tasis, D.; Tagmatarchis, N.; Bianco, A.; Prato, M. *Chem. Rev.* **2006**, *106*, 1105.
(9) (a) Hwang, K. C. *J. Chem. Soc., Chem. Commun.* **1995**, *2*, 173. (b) Mawhinney, D. B.; Naumenko, V.; Kuznetzova, A.; Yates, Y. T., Jr. *J. Am. Chem. Soc.* **2000**, *122*, 2383. (c) Banerjee, S.; Hemraj-Benny, T.; Wong, S. S. *Adv. Mater.* **2005**, *17*, 17.
(10) Shelimov, K. B.; Esenaliev, R. O.; Rinzler, A. G.; Huffman, C. B.; Smalley, R. E. *Chem. Phys. Lett.* **1998**, *282*, 429.
(11) Zhang, Y.; Shi, Z.; Gu, Z.; Iijima, S. *Carbon* **2000**, *38*, 2055.
(12) (a) Murakami, H.; Nakashima, N. *J. Nanosci. Nanotechnol.* **2006**, *6*, 16. (b) Star, A.; Liu, Y.; Grant, K.; Ridvan, L.; Stoddart, J. F.; Steuerman, D. W.; Diehl, M. R.; Boukai, A.; Heath, J. R. *Macromolecules* **2003**, *36*, 553.
(13) (a) Nakashima, N.; Tomonari, Y.; Murakami, H. *Chem. Lett.* **2002**, *31*, 638. (b) Guldi, D. M.; Rahman, G. M. A.; Jux, N.; Tagmatarchis, N.; Prato, M. *Angew. Chem., Int. Ed.* **2004**, *43*, 5526. (c) Chen, R. J.; Zhang, Y.; Wang, D.; Dai, H. *J. Am. Chem. Soc.* **2001**, *123*, 3838. (d) Angelez-Herranz, M.; Ehli, C.; Campidelli, S.; Guttiérez, M.; Hug, G. L.; Ohkubo, K.; Fukuzumi, S.; Prato, M.; Martín, N.; Guldi, D. M. *J. Am. Chem. Soc.* **2008**, *130*, 66. (e) Ehli, C.; Rahman, G. M. A.; Jux, N.; Balbinot, D.; Guldi, D. M.; Paolucci, F.; Marcaccio, M.; Paolucci, D.; Melle-Franco, M.; Zerbetto, F.; Campidelli, S.; Prato, M. *J. Am. Chem. Soc.* **2006**, *128*, 11222. (f) Bahun, G. J.; Wang, C.; Adronov, A. *J. Polym. Sci. A: Polym. Chem.* **2006**, *44*, 1941. (g) Schulz-Drost, C.; Sgobba, V.; Gerhards, C.; Leubner, S.; Calderon, R. M. K.; Ruland, A.; Guldi, D. M. *Angew. Chem., Int. Ed.* **2010**, *49*, 6425. (h) Petrov, P.; Stassin, F.; Pagnoulle, C.; Jérôme, R. *Chem. Commun.* **2003**, 2904. (i) Georgakilas, V.; Tzitzios, V.; Gournis, D.; Petridis, D. *Chem. Mater.* **2005**, *17*, 1613. (j) Yuan, W. Z.; Sun, J. Z.; Dong, Y.; Häussler, M.; Yang, F.; Xu, H. P.; Qin, A.; Lam, J. W. Y.; Zheng, Q.; Tang, B. Z. *Macromolecules* **2006**, *39*, 8011. (k) Meuer, S.; Braun, L.; Zentel, R. *Macromol. Chem. Phys.* **2009**, *10*, 1528. (l) Sandanayaka, A. S. D.; Chitta, R.; Subbaiyan, N. K.; D'Souza, L.; Ito, O.; D'Souza, F. *J. Phys. Chem. C* **2009**, *113*, 13425. (m) Maligaspe, E.; Sandanayaka, A. S. D.; Hasobe, T.; Ito, O.; D'Souza, F. *J. Am. Chem. Soc.* **2010**, *132*, 8158.
(14) (a) Zhang, J.; Lee, J.-K.; Wu, Y.; Murray, R. W. *Nano Lett.* **2003**, *3*, 403. (b) Satishkumar, B. C.; Brown, L. O.; Gao, Y.; Wang, C.-C.; Wang, H.-L.; Doorn, S. K. *Nat. Nanotechnol.* **2007**, *2*, 560.
(15) (a) Murakami, H.; Nomura, T.; Nakashima, N. *Chem. Phys. Lett.* **2003**, *378*, 481. (b) Li, H.; Zhou, B.; Lin, Y.; Gu, L.; Wang, W.; Fernando, K. A. S.; Kumar, S.; Allard, L. F.; Sun, Y.-P. *J. Am. Chem. Soc.* **2004**, *126*, 1014. (c) Satake, A.; Miyajima, Y.; Kobuke, Y. *Chem. Mater.* **2005**, *17*, 716. (d) Cheng, F.; Adronov, A. *Chem.—Eur. J.* **2006**, *12*, 5053. (e) Sgobba, V.; Rahman, G. M. A.; Guldi, D. M.; Jux, N.; Campidelli, S.; Prato, M. *Adv. Mater.* **2006**, *18*, 2264.
(16) (a) de la Torre, G.; Claessens, C. G.; Torres, T. *Chem. Commun.* **2007**, 2000. (b) Rio, Y.; Rodriguez-Morgade, M. S.; Torres, T. *Org. Biomol. Chem.* **2008**, *6*, 1877. (c) de la Torre, G.; Bottari, G.; Hahn, U.; Torres, T. *Struct. Bonding (Berlin)* **2010**, *135*, 1.

$ZnCl_2$ in refluxing *o*-dichlorobenzene (*o*-DCB)/dimethylformamide (DMF) (Scheme 1).

Additional experimental details are given in the Supporting Information.

Results and Discussion

Characterization of H_2Pc-Py/ZnPc-Py. The spectroscopic characterizations of the two lead compounds, namely, H_2Pc-Py and ZnPc-Py, were carried out in the following solvents/solvent mixtures: tetrahydrofuran (THF) and DMF as well as a mixture of 25% THF and 75% DMF. Metal-free tetra-*tert*-butylphthalocyanine (H_2Pc), the corresponding zinc complex (ZnPc), and 1-pyrenemethanol (Py) were used as internal references.

The absorption spectra of H_2Pc-Py and ZnPc-Py in THF show features of both building blocks, that is, pyrene and H_2Pc/ZnPc, with their corresponding characteristic signatures at 328/345 (Py), 366/680 (ZnPc-Py), and 366/668 and 702 nm (H_2Pc-Py). The H_2Pc/ZnPc maxima correlate to the corresponding Soret and Q-band absorptions.

In light of the strong and long-lived fluorescence features of H_2Pc, ZnPc, and Py moieties, their quantum yields and lifetimes were determined in the references as well as in H_2Pc-Py and ZnPc-Py. To this end, we focused on the selective excitation of Py and H_2Pc/ZnPc components at 275 and 610 nm, respectively, in THF. In particular, excitation of the Py reference leads to a fluorescence spectrum showing maxima in the blue part of the solar spectrum at 374 and 395 nm, a fluorescence quantum yield close to unity, and a fluorescence lifetime of nearly 100 ns.[13d] Turning to the excitation of the H_2Pc and ZnPc moieties at 610 nm, the following features were recorded in the red part of the solar spectrum. For ZnPc-Py we found a maximum at 683 nm and a shoulder at 745 nm, while H_2Pc-Py showed an intense peak at 706 nm with shoulders at 666, 733, and 777 nm in THF. In ZnPc-Py and H_2Pc-Py, excitation of Py at 275 nm gave rise to strong, almost quantitative quenching of the pyrene fluorescence features by 99%. A different situation is observed in the red part of the spectrum. Here, despite the Py excitation, either the H_2Pc- or the ZnPc-centered features are registered. Note the overlapping absorption features of Py and H_2Pc/ZnPc components in the 250−350 nm region.

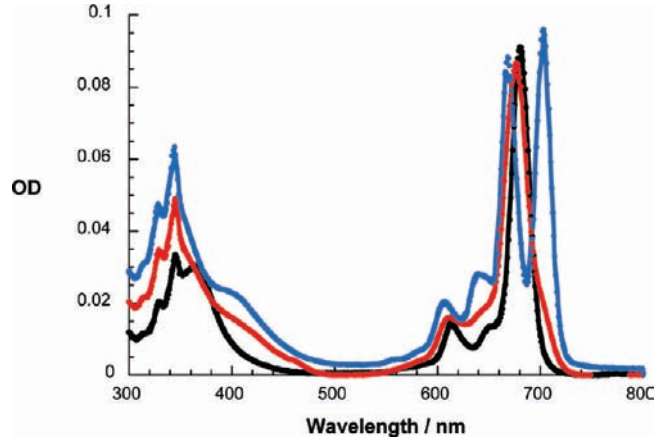

Figure 1. Absorption spectra of ZnPc-Py in DMF (black spectrum), H_2Pc-Py in DMF (red spectrum), and H_2Pc-Py in THF (blue spectrum).

Nevertheless, such a trend suggests an energy-transfer scenario from the energetically higher lying Py singlet excited state to the energetically lower lying H_2Pc/ZnPc singlet excited state. An excitation spectrum, that is, monitoring the Pc fluorescence features at varied excitation wavelengths, confirms this assumption by revealing features that track the absorption spectra of H_2Pc-Py and ZnPc-Py, including the characteristics of Py and H_2Pc/ZnPc components.

Important for the further characterization is the fact that the absorption spectra of ZnPc-Py remain nearly unchanged in THF and DMF, with maxima at 277/345 (Py), 366 (ZnPc Soret band), and 680 nm (ZnPc Q-band), but notable changes evolve for H_2Pc-Py. In THF, on one hand, the Q-band splits into two maxima at 668 and 702 nm, while in DMF, on the other hand, just one maximum is seen at 676 nm (Figure 1). This behavior has been previously observed[23,24] and attributed to the interaction of the basic center of DMF with the pyrrolic protons of the Pc, which produces a "symmetrization" of the molecule.[24] In other words, an electronic structure similar to the dianion-like species—characteristic for metallic complexes with D_{4h} symmetry—evolves. A notable but likewise weaker similarity is seen in the case of H_2Pc. Complementary investigations by means of steady-state and time-resolved fluorescence spectroscopy helped to confirm our assumption. In THF, ZnPc-Py and H_2Pc-Py revealed typical fluorescence features, namely distinct maxima at 683 and 706 nm, respectively. In DMF, no appreciable differences were noted for ZnPc-Py, whereas for H_2Pc-Py, in addition to the 706 nm peak, a second fluorescence peak evolved at 684 nm. The latter coincides with the fluorescence maximum of ZnPc-Py. This observation is in agreement with the formation of a dianion-like structure for H_2Pc-Py in DMF. Likewise, for H_2Pc, a similar trend is observed.

Considering that mixtures of THF and DMF were successfully used to prepare stable suspensions of SWNTs, we carried out a screening of the spectroscopic behavior of ZnPc-Py and H_2Pc-Py in different ratios of THF and DMF. For example, in a solvent mixture composed of 25 vol % THF and 75 vol % DMF, we find an intense Q-band absorption at 674 nm, accompanied by a weaker band at 702 nm for H_2Pc-Py. Mirror-imaging these

(17) (a) Soares, A. R. M.; Martínez-Díaz, M. V.; Bruckner, A.; Pereira, A. M. V. M.; Tomé, J. P. C.; Alonso, C. M. A.; Faustino, M. A. F.; Neves, M. G. P. M. S.; Tomé, A. C.; Silva, A. M. S.; Cavaleiro, J. A. S.; Torres, T.; Guldi, D. M. *Org. Lett.* **2007**, *9*, 1557. (b) Kameyama, K.; Satake, A.; Kobuke, Y. *Tetrahedron Lett.* **2004**, *45*, 7617.
(18) (a) D'Souza, F.; Ito, O. *Coord. Chem. Rev.* **2005**, *249*, 1410. (b) Gouloumis, A.; de la Escosura, A.; Vázquez, P.; Torres, T.; Kahnt, A.; Guldi, D. M.; Neugebauer, H.; Winder, C.; Drees, M.; Sariciftci, N. S. *Org. Lett.* **2006**, *8*, 5187.
(19) Kobayashi, N. *Coord. Chem. Rev.* **2002**, *227*, 129.
(20) (a) de la Torre, G.; Blau, W.; Torres, T. *Nanotechnology* **2003**, *14*, 765. (b) Xu, H. B.; Chen, H. Z.; Shi, M. M.; Bai, R.; Wang, M. *Mater. Chem. Phys.* **2005**, *94*, 342. (c) Ballesteros, B.; Campidelli, S.; de la Torre, G.; Ehli, C.; Guldi, D. M.; Prato, M.; Torres, T. *Chem. Commun.* **2007**, 2950. (d) Ballesteros, B.; de la Torre, G.; Ehli, C.; Rahman, G. M. A.; Agulló-Rueda, F.; Guldi, D. M.; Torres, T. *J. Am. Chem. Soc.* **2007**, *129*, 5061. (e) Yang, Z.; Pu, H.; Yuan, J.; Wan, D.; Liu, Y. *Chem. Phys. Lett.* **2008**, *465*, 73. (f) Campidelli, S.; Ballesteros, B.; Filoramo, A.; Diaz Díaz, D.; de la Torre, G.; Torres, T.; Rahman, G. M. A.; Ehli, C.; Kiessling, D.; Werner, F.; Sgobba, V.; Guldi, D. M.; Cioffi, C.; Prato, M.; Bourgoin, J. P. *J. Am. Chem. Soc.* **2008**, *130*, 11503. (g) He, N.; Chen, Y.; Bai, J.; Wang, J.; Blau, W. J.; Zhu, J. *J. Phys. Chem. B* **2009**, *113*, 13029.
(21) Bartelmess, J.; Ehli, C.; Cid, J.-J.; García-Iglesias, M.; Vázquez, P.; Torres, T.; Guldi, D. M. *Chem. Sci.* **2010**; in press.
(22) Ballesteros, B.; de la Torre, G.; Shearer, A.; Hausmann, A.; Herranz, M. A.; Guldi, D. M.; Torres, T. *Chem.—Eur. J.* **2010**, *16*, 114–125.
(23) (a) Nitschke, C.; O'Flaherty, S. M.; Kroll, M.; Blau, W. J. *J. Phys. Chem. B* **2004**, *108*, 1287. (b) Esenpınar, A. A.; Bulut, M. *Dyes Pigm.* **2008**, *76*, 249.
(24) Stillman, M. J.; Nyokong, T. in *Phthalocyanines: Properties and Appliocations*; Leznoff, C. C., Lever, A. B. P., Eds.; VCH: Weinheim, 1989; p 139.

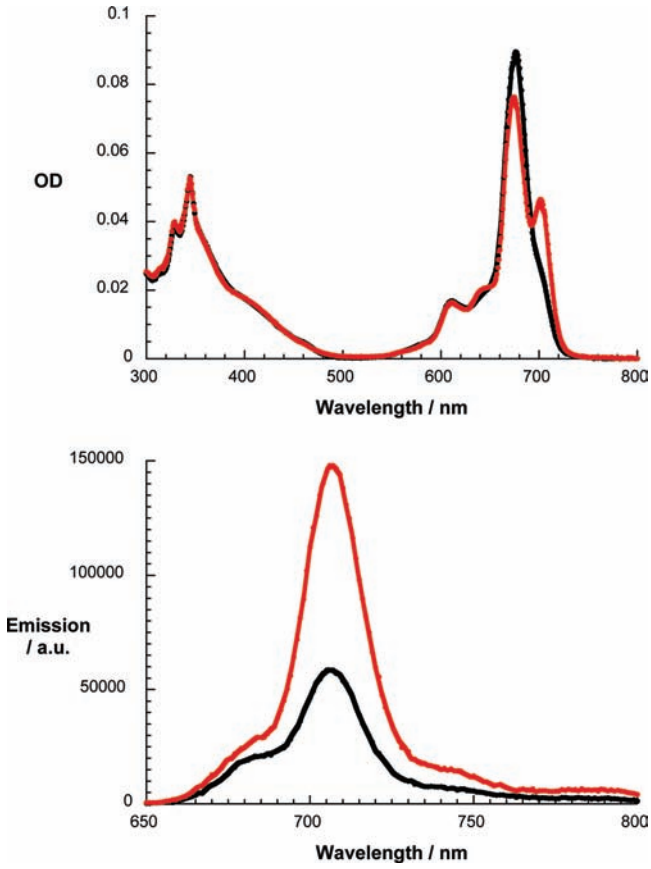

Figure 2. (Top) Absorption spectra of H_2Pc-Pc in DMF (black spectrum) and after addition of 3 vol % of H_2O (red spectrum). (Bottom) Fluorescence spectra of H_2Pc-Py in DMF (black spectrum) and DMF + 3 vol % H_2O (red spectrum).

absorption features, a single peak at 706 nm dominates the fluorescence spectrum of H_2Pc-Py. In addition, the fluorescence quantum yields and the fluorescence lifetimes (see Supporting Information, Table S1) change significantly in pure THF and DMF. Reassuring is the fact that values for the different DMF/THF mixtures are in between those seen for the pure solvents. The observations for H_2Pc are similar. The recovery of the splitting upon addition of THF can be rationalized considering that the presence of this solvent may disturb the interactions between DMF and the pyrrolic protons. In sharp contrast, ZnPc-Py as well as ZnPc is not susceptible to any solvent-related changes, including fluorescence quantum yields that are around 3.0 ns and fluorescence lifetimes that vary marginally between 2.9 and 3.5 ns.

As demonstrated, changes in the solvent environment exert rather large effects on the H_2Pc-Py absorptions. To follow up on this aspect, we started to perform titration assays with H_2Pc-Py in DMF and variable quantities of water.[25] In terms of absorption, the band at 676 nm decreases steadily and blue-shifts slightly, with the concomitant formation of a new band centered at 702 nm. In terms of fluorescence, the intensity of the peak at 706 nm increases by a factor of almost 3 when 3 vol % of water is present (Figure 2), and the fluorescence lifetime decreases with a strong reduction of the weight of the fast component (Table S1). A plausible explanation for these observations is that the presence of water disrupts the interactions between the basic center of the DMF and the pyrrolic protons. When, however, more water is added to the solution of H_2Pc-Py in DMF, a broad and blue-shifted band (630 nm) evolves, which is a signature of aggregates in protic media.

Next, the electrochemical and spectroelectrochemical features of Py, ZnPc, H_2Pc, ZnPc-Py, and H_2Pc-Py were explored. All of the measurements were performed in dichloromethane (DCM) containing tetrabutylammonium hexafluorophosphate (0.2 M) as electrolyte. Under oxidative conditions, Py shows a single oxidation at 1.17 V (vs. Fc/Fc^+), while for ZnPc and H_2Pc, oxidations evolved at 0.43/1.13 and 0.52/0.77/1.23 V (vs. Fc/Fc^+), respectively. ZnPc-Py and H_2Pc-Py are best described as the superimposition of their of Py and ZnPc or Py and H_2Pc components, with, however, some minor shifts, which are probably derived from the different substitution patterns. In particular, for ZnPc-Py, on one hand, oxidation processes are registered at 0.61, 1.10, and 1.26 V, and for H_2Pc-Py, on the other hand, the values are 0.8, 0.97, 1.19, and 1.36 V. As a complement to the electrochemical features, the spectroelectrochemical features were determined. To this end, absorption spectra were recorded without and with applying a potential. In the case of ZnPc and ZnPc-Py, the potentials were increased incrementally to 0.7 V. Working with H_2Pc required the application of potentials of up to 0.8 V, and a potential of 1.0 V was finally applied for H_2Pc-Py. Notable is that, under oxidative conditions, the ground-state absorption features fade away, with the concomitant growth of new bands. The latter represent the absorptions due to the formation of the one-electron-oxidized form of either ZnPc or H_2Pc. In detail, for ZnPc and ZnPc-Py, new bands are discernible in the 400−600 nm range and around 840 nm. These are the well-known fingerprints of the one-electron-oxidized form of ZnPc (see Supporting Information, Figure S1).[26] For H_2Pc and H_2Pc-Py, a broad absorption in the 400−600 nm range (i.e., H_2Pc, maxima at 405 and 535 nm; H_2Pc-Py, maximum at 490 nm) is observable; additionally, we can identify a band around 900 nm for both metal-free phthalocyanines.

The aforementioned assays were complemented by transient absorption measurements. For ZnPc in THF, the following changes occur upon 387 nm photoexcitation: The singlet excited state is formed right after the laser pulse. It comprises a broad transient maximum that is centered at 490 nm, followed by bleaching between 610 and 685 nm. This transient decays rather slowly on the time scale of our instrumental detection (i.e., 3.0 ns) due to intersystem crossing to the corresponding triplet manifold. The main spectral features of the latter are a maximum at 500 nm and a minimum at 680 nm. At this point we conclude that, especially in the near-infrared region, the two transients, namely, the singlet and the triplet excited state, differ largely in their absorption. Likewise, when exciting ZnPc-Py or H_2Pc-Py at 387 nm in a mixture of 25% THF/75% DMF, the transient bleach is discernible (Figure 3). To be precise, minima evolve for ZnPc-Py at 612/679 nm and for H_2Pc-Py at 609/677 nm. In contrast to additional experiments with 660 nm photoexcitation, a very fast S_2-to-S_1 conversion is seen, with rate constants around 1.4×10^{12} s^{-1} in the case of 387 nm excitation. The bleach is further accompanied by the formation of several new,

(25) Important in this context is that the DMF used in the experiments was from a recently opened, spectrophotometric grade bottle, with less than 0.15% H_2O.

(26) (a) Nyokong, T.; Gasyna, Z.; Stillman, M. J. *Inorg. Chem.* **1987**, *26*, 548. (b) El-Khouly, M. E.; Ito, O.; Smith, P. M.; D'Souza, F. *J. Photochem. Photobiol. C* **2004**, *5*, 79. (c) Kahnt, A.; Quintiliani, M.; Vázquez, P.; Guldi, D. M.; Torres, T. *ChemSusChem* **2008**, *1*, 97.

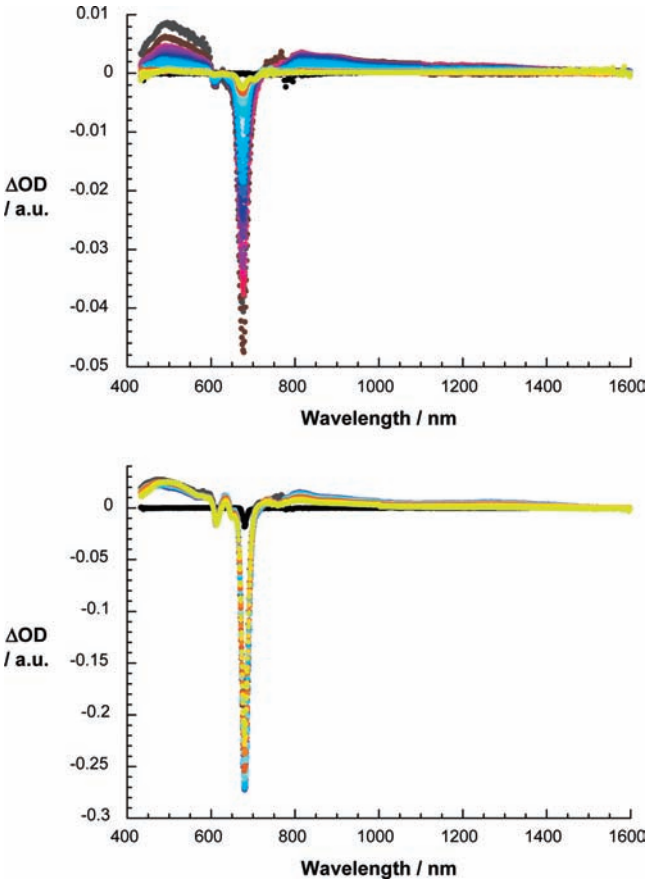

Figure 3. (Top) Differential absorption spectra (visible and near-infrared) obtained upon femtosecond flash photolysis (387 nm) of H_2Pc-Py in 25% THF/75% DMF with several time delays between 0 and 3000 ps at room temperature. (Bottom) Differential absorption spectra (visible and near-infrared) obtained upon femtosecond flash photolysis (387 nm) of ZnPc-Py in 25% THF/75% DMF with several time delays between 0 and 3000 ps at room temperature.

broad absorption bands in the ranges from 460 to 530 nm and from 780 to 960 nm. Py is not excited at either 387 or 660 nm excitation.

Titrations of SWNT suspensions with H_2Pc-Py/ZnPc-Py. The realization of novel SWNT hybrids, in which SWNTs are associated with H_2Pc/ZnPc by virtue of $\pi-\pi$ stacking, is the major thrust of the current work. To investigate the interactions between H_2Pc-Py/ZnPc-Py and SWNTs, titration experiments were carried out. First, semistable suspensions of SWNTs—containing finely dispersed SWNTs—were prepared in either THF or DMF. Here, 0.5 mg of solid SWNTs was added to 3 mL of THF or DMF, followed by a 10 min ultrasonication step. Three to four drops of this suspension were added to 10 mL of THF or DMF, followed by an additional 10 min of ultrasonication. This procedure is repeated up to 10 times to obtain a light-grayish semistable suspension of SWNTs. Care has been taken in handling the suspension and maintaining temperature stability as measures to prevent aggregation/precipitation of SWNTs. Decisive information for optimizing the dispersion of SWNTs was derived from absorption and fluorescence spectroscopy. As an example, attention was given to registering the SWNT-associated transitions—as they occur between different van Hove singularities in the density of states—in the near-infrared at 1090, 1171, 1318, and 1455 nm. In pure THF or DMF, it was impossible to perform several sonication and centrifugation cycles to separate fully individualized SWNTs from thinner and/or thicker bundles. Accordingly, attempts to map the steady-state fluorescence of SWNTs with white light were unsuccessful due to low SWNT concentrations. Appreciable SWNT band-gap fluorescence was detected only upon more intense laser excitation with the second harmonic generation of a Nd/YAG laser at 532 nm. Under these conditions, fluorescence maxima at 1120, 1278, 1422, and 1521 nm correlate well with the aforementioned absorption maxima (see Supporting Information, Figure S2).

These SWNT suspensions in THF were titrated with variable amounts of dissolved H_2Pc-Py and ZnPc-Py, bringing about drastic changes in absorption and fluorescence of the Pc component. First, the presence of SWNTs is manifested as a significant broadening of the H_2Pc and ZnPc features, especially in the Q-band region. Second, the absorption bands of the latter red-shift from 684 to 704 nm and from 668/702 to 699/725 nm for H_2Pc-Py in DMF (see Supporting Information, Figure S3). Third, in steady-state fluorescence experiments, the H_2Pc-Py- and ZnPc-Py-related features are quantitatively quenched until free, unbound H_2Pc-Py/ZnPc-Py remains in solution. Fourth, the near-infrared absorption transitions, which are associated with SWNTs, also undergo successive red-shifts of, on average, 4 nm. Finally, SWNTs fluoresce red-shifted (i.e., 1128, 1287, 1434, and 1543 nm) and quenched (vide infra, see also Figure S2). Taking these observations together, we reach the conclusion that H_2Pc-Py and ZnPc-Py were successfully immobilized onto SWNT. Regarding H_2Pc and ZnPc, the lack of anchor groups fails to give rise to any notable interactions (see Supporting Information, Figure S4).

The changes when adding an excess of H_2Pc-Py in DMF to predispersed SWNTs are interesting. In particular, we note that the Q-band maximum at 676 nm in DMF splits into two maxima at 671 and 702 nm, a trend that resembles the transformation seen when going from DMF to THF. Similarly, the fluorescence of H_2Pc-Py is affected, where the long-wavelength transition at 684 nm disappears and the fluorescence intensity increases, in line with the results found when going from DMF to THF. Due to self-absorption of the SWNT suspension and the quenching of the fluorescence of H_2Pc-Py immobilized onto SWNTs, quantification of this rise is not possible without major errors. In test experiments with H_2Pc—lacking Py—the changes in absorption and fluorescence were reproduced but without the aforementioned broadening of the absorption and the strong fluorescence quenching. Instead, the resulting absorption spectra are best described as linear combinations of the individual features (i.e., H_2Pc and SWNTs; see Figures S3 and S4).

Preparation of Stable SWNT Suspensions. Working at higher concentrations, the association between H_2Pc-Py/ZnPc-Py and SWNTs is too weak to stabilize individual SWNTs and to avoid bundle formation. To circumvent the issues of instability and concentration, a mixture of 25 vol % THF and 75 vol % DMF was utilized since, in these conditions, SWNTs can be readily dispersed in high concentrations. In the present context, we used 0.5 mg of solid SWNTs that were quantitatively dispersed in 10 mL of the solvent. After ultrasonication, which never exceeded 20 min, we obtained a homogeneous, dark gray suspension of SWNTs. Significantly, any excess of SWNTs was removed by centrifugation for 15 min at 9.6 kG. The resulting SWNT suspensions did not show appreciable SWNT-based fluorescence in the NIR, since most likely, debundling is incomplete. Nevertheless, their overall stability renders them an ideal starting point for further tests.

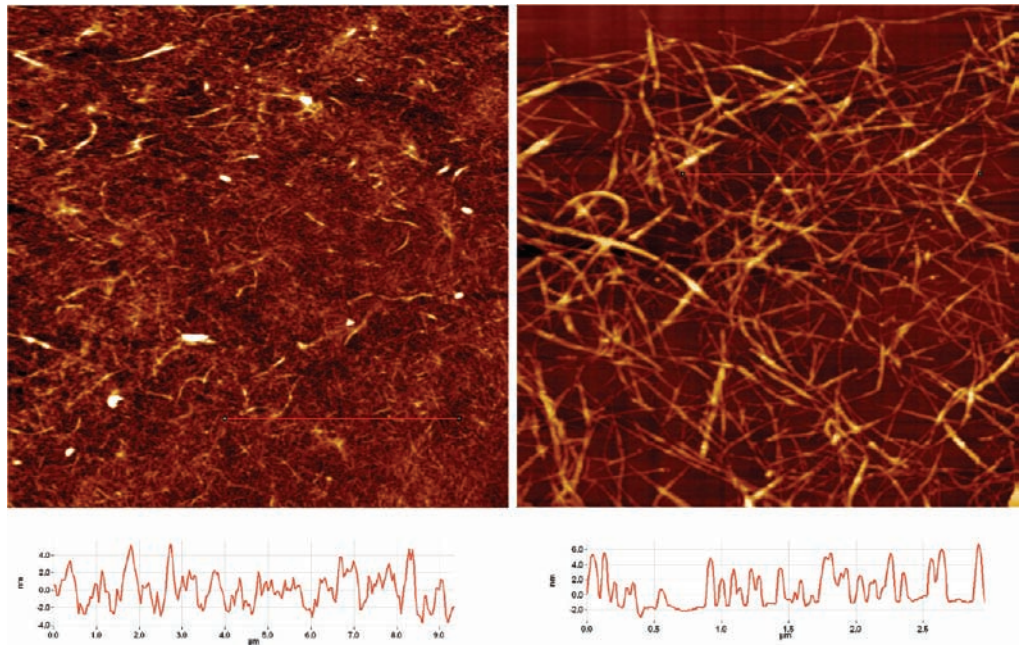

Figure 4. (Left) AFM image of ZnPc-Py/SWNT dispersion, spin-coated on a Si slide (20 × 20 μm). (Right) AFM image of H_2P-Py/SWNT dispersion, spin-coated on a Si slide (5 × 5 μm).

Following the aforementioned procedure, solutions of H_2Pc-Py/ZnPc-Py in 25 vol % THF and 75 vol % DMF afforded stable suspensions of H_2Pc-Py/SWNT or ZnPc-Py/SWNT. Depending on the ratio of H_2Pc-Py to SWNT and ZnPc-Py to SWNT, features of immobilized and also free H_2Pc-Py and ZnPc-Py were dissected. The earlier are seen in the form of red-shifted Q-band absorptions at 704 nm for ZnPc-Py/SWNT, while proof for H_2Pc-Py/SWNT is built on maxima at 725 nm. The red-shifts seen for H_2Pc-Py in H_2Pc-Py/SWNT are the same throughout the titration experiments. We believe that both free and immobilized forms are in equilibrium, but with a slight tendency to favor the immobilized H_2Pc-Py/SWNT. The same applies to ZnPc-Py and ZnPc-Py/SWNT equilibrium. Regarding the overall stability of the different suspensions, we could not derive any differences between ZnPc-Py and H_2Pc-Py. The ZnPc/H_2Pc-centered fluorescence in ZnPc-Py/SWNT and H_2Pc-Py/SWNT is quenched by approximately 2 orders of magnitude when compared to those of ZnPc-Py and H_2Pc-Py in the absence of any SWNTs. Owing to the immobilization onto SWNTs, the fluorescence is quenched, but competitive light absorption due to the presence of SWNTs might also contribute.

Atomic force microscopy of the dispersed H_2Pc-Py/SWNT or ZnPc-Py/SWNT was carried out to ensure the homogeneity of the corresponding suspensions. In Figure 4, typical AFM images are shown. They confirm, the H_2Pc-Py/SWNT and ZnPc-Py/SWNT throughout the scanned area, the presence of well-dispersed thin bundles of SWNTs with diameters between 2 and 6 nm and a length of around 5 μm.

More insight into interactions of H_2Pc-Py/ZnPc-Py with SWNTs was gathered by mapping the band-gap fluorescence of SWNTs upon lamp irradiation at varying wavelengths. First, a SWNT/ sodium dodecylbenzenesulfonate (SDBS) suspension in D_2O was prepared as an internal standard to be compared with H_2Pc-Py/SWNT or ZnPc-Py/SWNT. Figures 5 −7 compare the fluorescence spectra of SWNT/SDBS in D_2O with those of H_2Pc-Py/SWNT or ZnPc-Py/SWNT in 25 vol % THF and 75 vol % DMF. All suspensions exhibit the same optical density at different excitation wavelengths. The fact that different

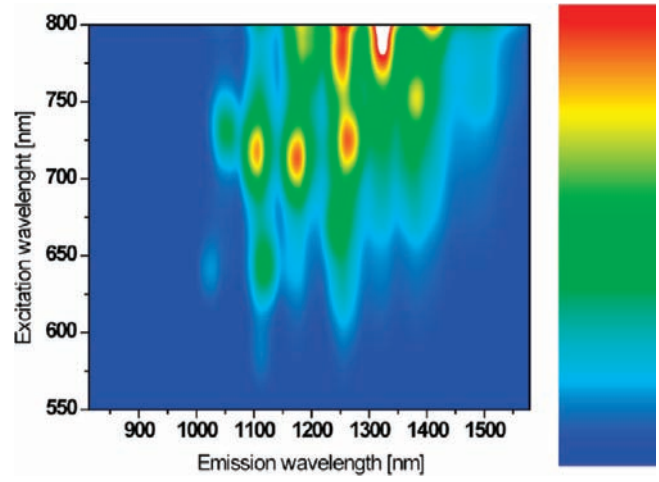

Figure 5. Steady-state fluorescence spectra—with increasing intensity from blue to green to yellow and to red—of SWNT/SDBS in D_2O dispersion.

solvents were used should not influence the overall interpretation. SWNT/SDBS exhibits the strongest fluorescence maxima, ascribed to (9,4), (7,6), (8,6), (11,3), (9,5), (10,5), (8,7), and (9,7).[27] A closer look at the fluorescence features following excitation at 725 nm (see Figure 8) shows that all SWNT-centered fluorescence of ZnPc-Py/SWNT and H_2Pc-Py/SWNT is red-shifted and strongly quenched (i.e., SDBS/SWNT/D_2O, 1055, 1108, 1178, 1267, (1327), 1382, 1484 nm; ZnPc-Py/SWNT: 1081, 1108, 1213, 1297, 1413, 1535 nm; H_2Pc-Py/SWNT: 1184, 1141, 1219, 1303, 1431, 1543 nm). In other words, average red-shifts of 33 and 41 nm emerge for ZnPc-Py/SWNT and H_2Pc-Py/SWNT relative to SWNT/SDBS in D_2O. Apparently, larger diameter SWNTs are subject to stronger red-shifts than smaller diameter SWNTs. These findings further confirm the successful immobilization.[28] When analyzing the

(27) Specific SWNTs were assigned to fluorescence bands by using the Horiba Jobin Yvon Nanosizer version 2.0.

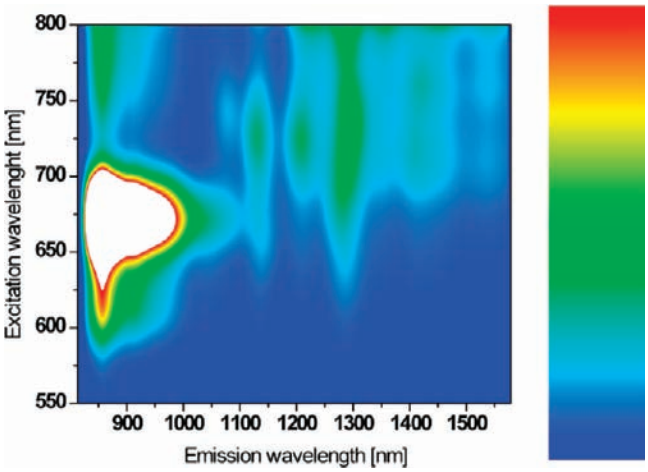

Figure 6. Steady-state fluorescence spectra—with increasing intensity from blue to green to yellow and to red—of ZnPc-Py/SWNT in 25% THF/75% DMF dispersion.

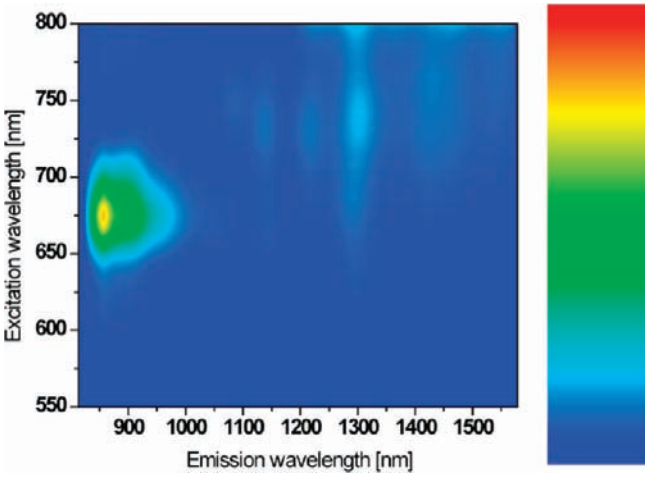

Figure 7. Steady-state fluorescence spectra—with increasing intensity from blue to green to yellow and to red—of H_2Pc-Py/SWNT in 25% THF/75% DMF dispersion.

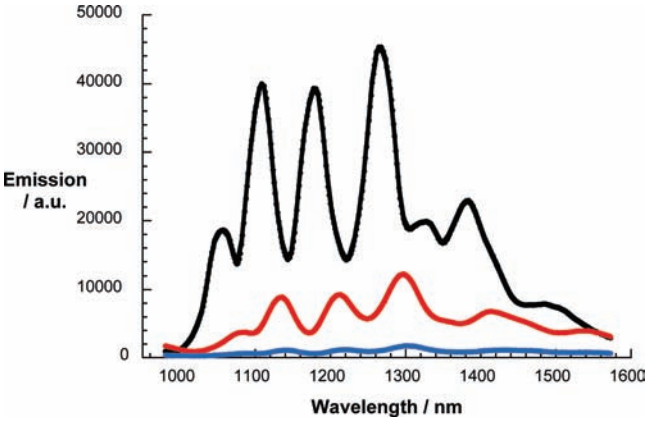

Figure 8. Comparison of the NIR fluorescence spectra of SWNT/SDBS in D_2O (black), ZnPc-Py/SWNT in 25% THF/75% DMF (red), and H_2Pc-Py/SWNT in 25% THF/75% DMF (blue) upon lamp excitation at 725 nm.

fluorescence intensity throughout the selected range, we observe an average quenching of 70% for ZnPc-Py/SWNT and 95% for H_2Pc-Py/SWNT. From the latter we conclude that H_2Pc-Py/SWNT shows the strongest interactions, a trend that is in perfect agreement with the extent of red-shifts seen in the absorption spectra. Laser excitation at 532 nm was carried out to verify the quenching and red-shifting of the SWNT fluorescence bands. Considering the aforementioned, immobilization of ZnPc-Py or H_2Pc-Py onto SWNTs is mainly responsible for the quenching of SWNT fluorescence.

To probe the electronic and structural influence that the immobilization of H_2Pc-Py/ZnPc-Py onto SWNTs might exert, Raman measurements were performed with liquid samples as well as solid samples (i.e., dried on a glass slide) with an excitation wavelength of 1064 nm. The D-band at 1278 cm^{-1}, as a reflection of sp^2-hybridization due to rupture in the SWNT structure or chemical changes of the SWNTs, was quite weak for all of the samples.[29] Moreover, the fact that there is essentially no difference in intensity between, for example, SWNTs and H_2Pc-Py/SWNT attests to the absence of structural damage of the SWNT structure as a result of our workup procedure. This observation is well in line with recently published studies on the effects of ultrasonication on SWNTs.[30] Likewise, no changes are seen when the G-band at 1591 cm^{-1} and the G′-band at 2548 cm^{-1} in H_2Pc-Py/SWNT and in SWNTs are compared either in the solid state or in suspensions (i.e., 25% THF/75% DMF).[31] Similar results were gathered for ZnPc-Py/SWNT.

Transient absorption spectroscopy was employed to confirm the ultrafast singlet excited-state deactivations and, in addition, to characterize the nature of the photoproducts. The same ZnPc singlet excited characteristics—despite the presence of the electron-accepting SWNTs—were registered upon 387 nm photoexcitation of ZnPc-Py/SWNT (see Supporting Information, Figure S5, and Figure 9). This confirms the successful excitation of ZnPc. In contrast to the slow intersystem crossing which was noted for ZnPc and ZnPc-Py, the ZnPc singlet excited-state features now decay rather quickly. The lifetimes (i.e., 3 ps) reflect the global trends seen in the fluorescence experiments. Simultaneously with the ZnPc singlet excited-state decay, the formation of a new transient species evolves with distinct maxima at 520 and 840, which are attributes of the one-electron-oxidized ZnPc radical cation. Similarly, the range beyond 1000 nm (i.e., 1000−1600 nm) is important, which immediately after the photoexcitation is dominated by a negative imprint of the van Hove singularities of SWNTs. Notable are appreciable blue-shifts of the transient bleaches, which represent the formation of a new product, with minima that shift from 1151, 1286, 1448, and 1582 nm to 1137, 1280 1428, and 1562 nm, respectively.

(28) (a) Bachilo, S. M.; Strano, M. S.; Kittrell, C.; Hauge, R. H.; Smalley, R. E.; Weisman, R. B. *Science* **2002**, *298*, 2361. (b) O'Connell, M. J.; Bachilo, S. M.; Huffman, C. B.; Moore, V. C.; Strano, M. S.; Haroz, E. H.; Rialon, K. L.; Boul, P. J.; Noon, W. H.; Kittrell, C.; Ma, J.; Hauge, R. H.; Weisman, R. B.; Smalley, R. E. *Science* **2002**, *297*, 593. (c) Weisman, R. B.; Bachilo, S. M. *Nano Lett.* **2003**, *3*, 1235. (d) Hartschuh, A.; Pedrosa, H. N.; Novotny, L.; Krauss, T. D. *Science* **2003**, *301*, 1354. (e) Yoon, D.; Kang, S.-J.; Choi, J.-B.; Kim, Y.-J.; Baik, S. *J. Nanosci. Nanotechnol.* **2007**, *7*, 3727.
(29) (a) Eklund, P. C.; Holden, J. M.; Jishi, R. A. *Carbon* **1995**, *33*, 959. (b) Dresselhaus, M. S.; Jorio, A.; Souza Filho, A. G.; Dresselhaus, G.; Saito, R. *Physica B* **2002**, *15*, 15. (c) Chen, G.; Sumanasekera, G. U.; Pradhan, B. K.; Gupka, R.; Eklund, P. C.; Bronikowski, M. J.; Smalley, R. E. *J. Nanosci. Nanotechnol.* **2002**, *2*, 621. (d) Dresselhaus, M. S.; Dresselhaus, G.; Saito, R.; Jorio, A. *Phys. Rep.* **2005**, *409*, 47. (e) Lefrant, S.; Baltog, I.; Baibarac, M. *Synth. Met.* **2009**, *159*, 2173.
(30) Forney, M. W.; Poler, J. C. *J. Am. Chem. Soc.* **2010**, *132*, 791.
(31) (a) Maciel, I. O.; Anderson, N.; Pimento, M. A.; Hartschuh, A.; Qian, H.; Terrones, M.; Terrones, H.; Campos-Delgado, J.; Rao, A. M.; Novotny, L.; Jorio, A. *Nat. Mater.* **2008**, *7*, 878. (b) Dresselhaus, M. S.; Jorio, A.; Hofmann, M.; Dresselhaus, G.; Saito, R. *Nano Lett.* **2010**, *10*, 751.

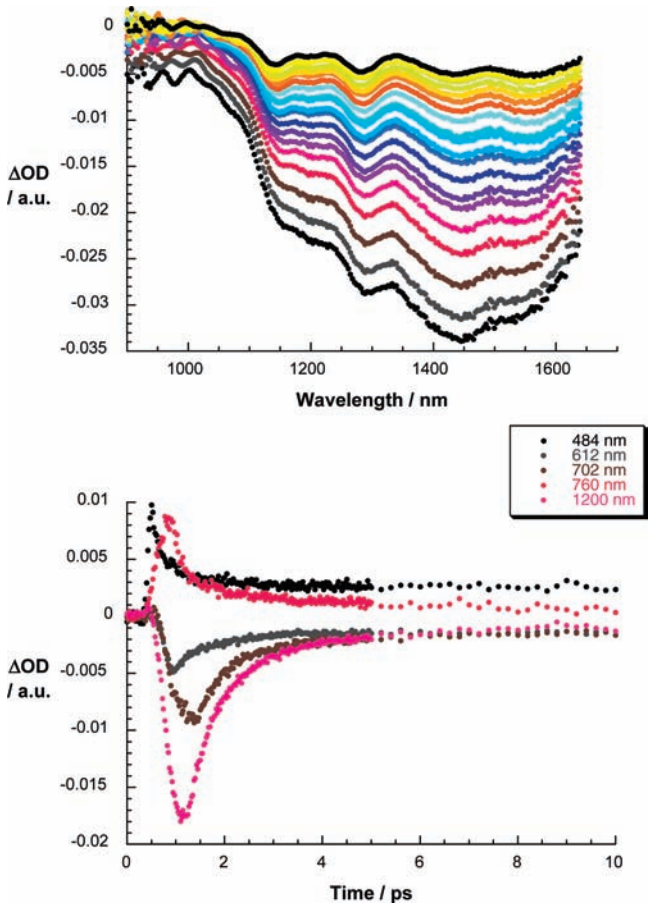

Figure 9. (Top) Differential absorption spectra (extended near-infrared) obtained upon femtosecond flash photolysis (387 nm) of ZnPc-Py/SWNT with several time delays between 0 and 10 ps at room temperature. (Bottom) Time−absorption profiles of spectra shown above at 484, 612, 702, 760, and 1200 nm, monitoring the charge separation.

Implicit are new conduction band electrons, injected from photoexcited ZnPc, shifting the SWNT transitions to lower energies. Thus, we reach the conclusion that photoexcitation of ZnPc-Py/SWNT is followed by a rapid charge transfer. A multiwavelength analysis of the newly developed charge-transfer state reveals its metastable character with decays beyond the 3.0 ns time window of our experimental setup.

The apparent equilibrium between immobilized and free H_2Pc-Py/ZnPc-Py was further tested in a series of follow-up experiments. First, dilution experiments were the focus of our investigations. The addition of extra solvent to the suspensions of H_2Pc-Py/SWNT or ZnPc-Py/SWNT led to a notable linear decrease of the absorption fingerprints of the Pc Q-bands representing immobilized H_2Pc-Py/ZnPc-Py and the concomitant increase of the absorptions corresponding to free H_2Pc-Py/ZnPc-Py species.

Second, additions of a nonionic surfactant (i.e., Triton X-100) were tested as a powerful means to replace H_2Pc-Py/ZnPc-Py, which is immobilized onto the surface of SWNTs. As important reference experiments, ZnPc and ZnPc-Py were found to be insusceptible to notable changes in terms of their absorption and fluorescence spectra, fluorescence quantum yield, and fluorescence lifetime—in a solvent mixture containing 25 vol % THF, 75 vol % DMF, and 5 vol % Triton X-100. In contrast, the experiments with H_2Pc and H_2Pc-Py showed an explicit influence of Triton X-100 on the characteristics of the system. The absorption spectrum of H_2Pc still reveals the weak band at 695 nm, while the absorption of H_2Pc-Py is essentially a mirror image of that established for the H_2Pc-Py in pure dry DMF. Under the same conditions (i.e., 25 vol % THF, 75 vol % DMF, and 5 vol % Triton X-100), the fluorescence pattern of H_2Pc reveals two symmetrical fluorescence bands at 671 and 700 nm. Notably, in the absence of Triton X-100, the band at 700 nm dominates, and for H_2Pc-Py (in the presence of Triton-X-100), the band at 706 nm disappeared completely, leaving just the weak fluorescence band at 682 nm. The H_2Pc-centered fluorescence quantum yields tend to be much lower in the presence of Triton X-100. For example, the quantum yields drop for H_2Pc from 0.40 to 0.15 and for H_2Pc-Py from 0.18 to 0.03. In concentration-dependent experiments, in which the Triton X-100 concentration was incrementally increased to a maximum of 5 vol %, the aforementioned changes were further corroborated. Turning to ZnPc-Py/SWNT, the alterations upon the addition of Triton X-100 include a decrease of the absorption signature of the immobilized form (i.e., ZnPc-Py/SWNT), an increase of the absorption signature associated with the free form (i.e., ZnPc-Py), and an increase of the overall fluorescence intensity (i.e., ZnPc-Py). A similar trend is observed for H_2Pc-Py/SWNT in the presence of Triton X-100 (vide supra). Support for this notion came from the recovery of the absorption features known from the free form of H_2Pc-Py (in 25 vol % THF, 75 vol % DMF, and 5 vol % Triton X-100) and that go along with decreasing intensity of the 706 nm fluorescence and increasing intensity of the 682 nm fluorescence.[32]

Finally, we explored the influence of 1,4-diazabicyclo-[2.2.2]octane (DABCO), a bidendate ligand that coordinates strongly (10^5 M^{-1}) to ZnPc, on the equilibrium.[33] Crucial for our assays is that the addition of DABCO to ZnPc or ZnPc-Py has no profound impact on the fluorescence quantum yield. In fact, the quantum yields are 0.27 and 0.25 for ZnPc without and with DABCO, respectively. For ZnPc-Py, the corresponding values are 0.31 and 0.25. Equally important is the observation that the fluorescence lifetimes remain constant. Performing the same titration experiments with SWNT suspensions and addition of ZnPc-Py until a slight excess of ZnPc-Py is reached (Figure 10), the absorption of immobilized ZnPc-Py intensifies at the expense of that of free ZnPc-Py upon addition of DABCO. This indicates the immobilization of additional ZnPc-Py, which is bound to ZnPc-Py/SWNT by means of DABCO. Also, fluorescence features of the free form of the ZnPc-Py fade due to connection to the SWNT surface. All these occur exclusively for ZnPc-Py, since H_2Pc-Py/SWNT solutions are resistant owing to the lack of metal center.

Thin-Film Preparation and Characterization. After our success in debundling and immobilizing H_2Pc-Py/ZnPc-Py onto SWNTs, solid-state films were prepared. To this end, ZnPc-Py/SWNT suspensions were prepared in a solvent mixture of 25% THF/75% DMF following the above-described procedure. Always an excess of either H_2Pc-Py or ZnPc-Py was used to ensure a maximum loading on SWNT. In the first step of the preparation procedure, an indium tin oxide (ITO) slide was carefully cleaned in isopropanol and dried. The SWNT suspensions were then filtered by using a 0.2 μm PTFE-supported membrane filter. During the filtration, the excess of H_2Pc-Py or ZnPc-Py in solution was removed; the filtrate was of greenish

(32) Control experiments with SWNTs dispersed with the help of 5 vol % Triton X-100 failed to provide unambiguous evidence for the immobilization of either ZnPc-Py or H_2Pc-Py.
(33) Hunter, C. A.; Meah, M. N.; Sanders, J. K. M. *J. Am. Chem. Soc.* **1990**, *112*, 5773.

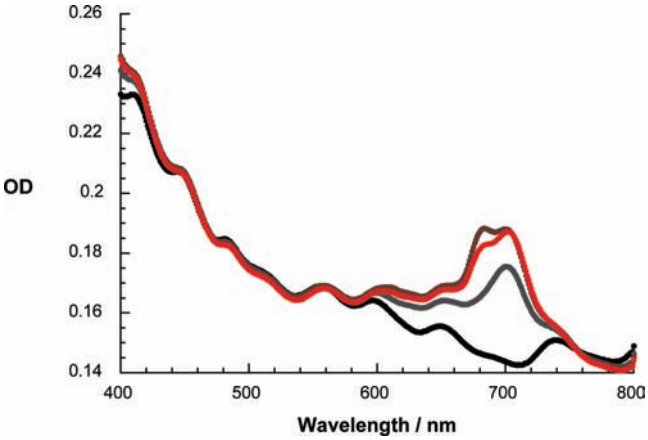

Figure 10. Absorption spectra of SWNTs in 25% THF/75% DMF (black spectrum), after addition of a small amount of ZnPc-Py solution (gray spectrum), after a second addition of ZnPc-Py solution (brown spectrum; note the presence of the absorption band of free ZnPc-Py at 680 nm), and after addition of 0.1 mg of solid DABCO (red spectrum).

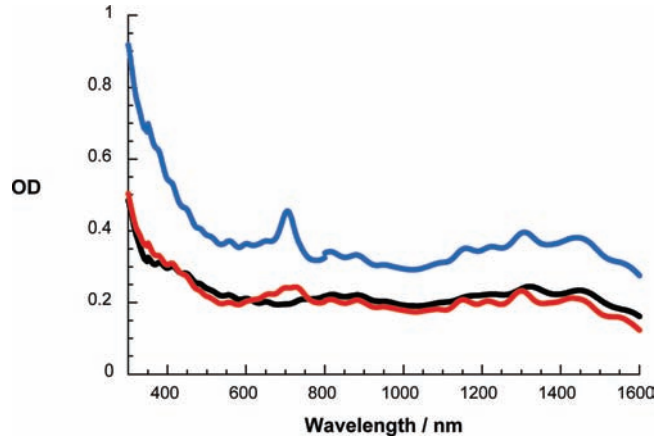

Figure 11. Absorption spectra of SWNT thin film (black spectrum), ZnPc-Py/SWNT thin film (blue spectrum), and H_2Pc-Py/SWNT thin film (red spectrum), all on cleaned ITO.

color. Owing to the equilibrium between bound and free H_2Pc-Py/ZnPc-Py, we were reluctant to excessively wash the resulting black films. The resulting SWNT films were carefully transferred to ITO and dried under low pressure for 20 min at 120 °C, leading to homogeneous SWNT films on ITO.[20f] Absorption spectroscopy was used to determine the optical density of the thin films and to ensure the presence of H_2Pc-Py/SWNT and ZnPc-Py/SWNT. In the case of ZnPc-Py/SWNT, we observed an intense Q-band absorption at 705 nm, which corresponds to ZnPc-Py immobilized onto SWNT. No absorption of free ZnPc-Py was detectable. Next to ZnPc-Py/SWNT, we also prepared films with H_2Pc-Py/SWNT, DABCO/ZnPc-Py/SWNT, and just SWNTs, all derived from solvent mixtures of 25% THF/75% DMF.

In all cases, high-quality films were produced. In DABCO/ZnPc-Py/SWNT and ZnPc-Py/SWNT, the absorptions—in particular those of ZnPc-Py—were quite similar. Importantly, H_2Pc-Py/SWNT shows features (i.e., Q-bands at 699 and 725 nm) that were established during the titration experiments. A closer inspection of the features in the NIR reveals a similar basic structure for ZnPc-Py/SWNT and H_2Pc-Py/SWNT, but with some differences. The most notable exception is that the absorption bands of H_2Pc-Py/SWNT are better resolved and blue-shifted relative to those of ZnPc-Py/SWNT. Incomplete SWNT debundling and the lack of resolution lead in the SWNT films to red-shifted and weak absorption features (Figure 11).

Solar Cell Fabrication. In the final part of our investigations, we manufactured prototype solar cells comprised of ZnPc-Py/SWNT or H_2Pc-Py/SWNT. The latter were deposited onto a 0.2 μm pore size PTFE filter from a suspension in 25% THF/752% DMF. Variable film thickness and, hence, increasing or decreasing absorptions are obtained by changing the filtered volume. Insight into the film morphology came from AFM and SEM measurements. SEM investigations show that the SWNTs homogeneously cover the substrate surface and form a membrane-like film (Figure 12). The SWNTs arrange in intertwined bundles with widths and lengths of around 10 nm and several hundreds of nanometers, respectively. AFM images (not shown) corroborate those observations with the presence of thicker bundles on the surface.

In the first sets of experiments, photocurrents were recorded for SWNT, ZnPc-Py/SWNT, and H_2Pc-Py/SWNT in the absence

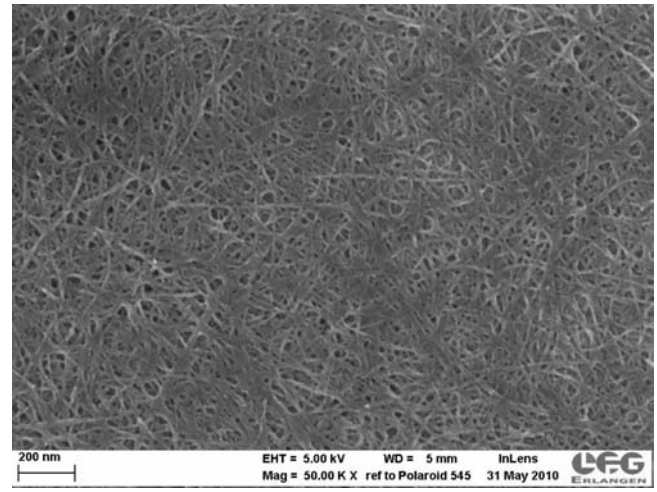

Figure 12. SEM image of H_2Pc-Py/SWNT thin film on ITO. 50000× magnification and an acceleration voltage of 5 kV.

and in the presence of an external bias under white-light illumination.[34] Photoanodic behavior was always observed under short-circuit conditions, which is indicative of photogenerated electrons that flow from the film to the ITO electrode. Comparing, however, the photoaction spectra of the different cells, that is, SWNTs, ZnPc-Py/SWNT, and H_2Pc-Py/SWNT, with I^-/I_2 (0.5 M/0.01 M) electrolyte revealed always the best performances for H_2Pc-Py/SWNT. In particular, maximum internal photoconversion efficiency (IPCE) values were 0.4% for SWNT, 0.75% for ZnPc-Py/SWNT, and 2.4% for H_2Pc-Py/SWNT for cells that exhibited the same optical absorption throughout the visible and near-infrared parts of the spectrum.

In light of the above results, we started to further optimize the H_2Pc-Py/SWNT cells. A major improvement in film quality came from refluxing the ITO slides in *n*-propanol for 1 h. This ensured the optimum hydrophobicity of ITO and, in turn, the deposition of H_2Pc-Py/SWNT. In addition, 0.5 M I^- and 0.1 M

(34) The electrochemical cell consists of SWNT-modified ITO and a Pt-coated FTO as a counter electrode. To achieve uniform deposition, a 5 mM solution of $H_2PtCl_6 \times H_2O$ in dry isopropanol is dispersed onto the slide. Successive heat treatment at 480 °C removes all additives, leaving only the pure Pt catalyst on the surface. Subsequently the SWNT/ITO and the Pt/FTO electrodes are melted together using Surlyn ionomer. The resulting 50 μm gap is filled with I^-/I_2 (0.5 M/0.1 M) as a redox mediator.

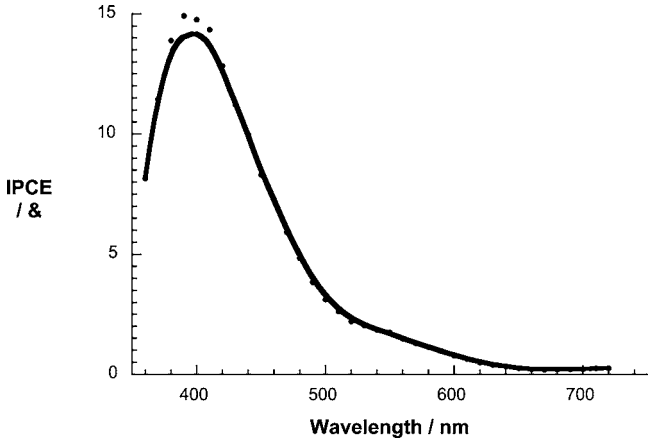

Figure 13. IPCE spectra of H_2Pc-Py/SWNT thin film in an I^-/I_2 (0.5 M/0.1 M) sandwich cell.

I_2 emerged as the best electrolyte concentrations for H_2Pc-Py/SWNT. Current−voltage measurements were then carried out in a voltage range between −0.5 V and +0.5 V at a rate of 5 mV/s. Around 26.6 or 53.4 mV for thinner and thicker films of 0.1 and 0.22 au, respectively, an open-circuit voltage sets in, where no appreciable currents flow, neither in the dark nor under illumination. Increasing the bias toward the anodic range resulted in an increase of photocurrent as a consequence of facilitated electron injection into ITO. These observations are consistent with the expected photooxidation of H_2Pc. At the maximum applicable bias—prior to any irreversible changes in the photoactive layer—the net currents, calculated by subtracting the dark currents from the photocurrents, were between 79 and 134 μA for 0.1 and 0.22 au, respectively. We noticed that the sign of the photocurrent reverted when cathodic biases were applied.

Next, the photoaction spectra for H_2Pc-Py/SWNT cells under monochromatic conditions were recorded and the IPCEs determined. In line with what has been noted in the absorption spectra, broad and featureless transitions emerge in the photoaction spectrum between 350 and 720 nm (Figures 11 and 13). The maximum IPCE values are intriguing, reach from 5 up to 15% without applied bias. When a bias of +0.1 V was applied, the derived IPCE values further increased to a maximum of 23%.

Conclusions

In this work, phthalocyanine−pyrene conjugates, ZnPc-Py and H_2Pc-Py, have emerged as valuable building blocks for assembling electron donor−acceptor hybrids with SWNTs. Owing to the strong ability of pyrene to adhere to SWNT sidewalls by means of $\pi-\pi$ interactions, we have exploited this polyaromatic anchor to immobilize metal-free (H_2Pc) as well as zinc (ZnPc) phthalocyanines onto the surface of SWNTs. To this end, the formation of stable ZnPc/SWNT and H_2Pc/SWNT suspensions has been unequivocally confirmed by means of diverse spectroscopic techniques. Most important in the characterization of the resulting assemblies are assays with respect to photoinduced electron-transfer events, from the singlet excited state of ZnPc or H_2Pc to SWNTs, as probed by steady-state emission studies and transient absorption spectroscopy.

Encouraged by such charge-transfer features, we have utilized ZnPc/SWNT and H_2Pc/SWNT thin films in photoelectrochemical cells to test their solar energy conversion potential. Performances have been realized that are much superior to those of previously reported SWNT conjugates and hybrids.[20f] In particular, H_2Pc-Py/SWNT thin films reveal stable and reproducible photocurrents with IPCE values as large as 15 and 23%, without and with an applied bias of +0.1 V, ranking among the highest reported values for SWNT-based systems. This result highlights the benefits of non-covalent approaches to the preparation of electron donor−acceptor hybrids in solar energy conversion schemes.

Acknowledgment. This work has been supported by the Spanish MEC (CTQ-2008-00418/BQU and CONSOLIDER INGENIO 2010, CSD2007-00010), the Comunidad de Madrid (MADRISOLAR-2, S2009/PPQ/1533), the COST Action D35, the University of Trieste, the Italian Ministry of Education MIUR (Cofin Prot. 20085M27SS), and Deutsche Forschungsgemeinschaft, Cluster of Excellence "Engineering of Advanced Materials", FCI, the Office of Basic Energy Sciences of the U.S. We are grateful to the Zentralinstitut für Neue Materialien und Prozesstechnik in Fürth for the possibility to perfom AFM measurements.

Supporting Information Available: Experimental section, fluorescence quantum yields and lifetimes of the different compounds in varied environments, spectroelectrochemistry of ZnPc-Py, and spectra of titrations of SWNT suspensions with H_2Pc-Py (absorption and NIR fluorescence) and H_2Pc (absorption). This material is available free of charge via the Internet at http://pubs.acs.org.

JA107131R